

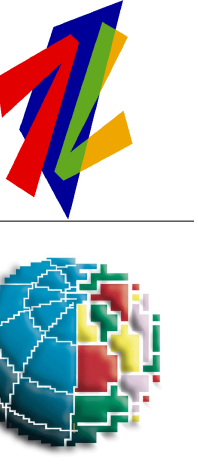
S53A-1034 M_{wpd} : Rapid Determination of Earthquake Magnitude and Tsunamigenic Potential from P Waveforms

Anthony Lomax

A Lomax Scientific, Mouans-Sartoux, France
anthony@alomax.net www.alomax.net

Alberto Michelini

Istituto Nazionale di Geofisica e Vulcanologia (INGV),
Roma, Italy michelini@ingv.it www.ingv.it



Summary

We present a duration-amplitude procedure for rapid determination (within 20 minutes of OT) of earthquake moment magnitude, M_{wps} , from P -wave recordings at teleseismic distances. The procedure determines apparent source durations, T_0 , from high-frequency, P -waveforms, and estimates moments by integration of broadband displacement waveforms over the interval t_P to $t_P + T_0$ where t_P is the P arrival time. Application to 79 recent, large earthquakes ($M_{w,CMT}$ 6.6 to 9.3) shows that scaling of the moment estimates for interplate thrust and possibly tsunami earthquakes is necessary to best match $M_{w,CMT}$. With this scaling, M_{wps} matches $M_{w,CMT}$ typically within ± 0.2 magnitude units and M_{wps} does not saturate for the largest events. The explicit use of the source duration, the moment scaling, and other characteristics of the duration-amplitude methodology make it an extension of the widely used M_{wp} rapid-magnitude procedure. The obtained durations and moments allow rapid estimation of the energy-to-moment ratio Θ for identification of tsunami earthquakes.

1. Introduction

Effective tsunami warning and emergency response for large earthquakes requires accurate knowledge of the event size within 30 minutes or less after the event origin time (OT). The 26 December 2004, M9 Sumatra-Andaman earthquake caused a tsunami that devastated coasts around the Eastern Indian Ocean within 3 hours; the 17 July 2006, M7.7 Java earthquake caused an unexpectedly large and destructive tsunami. For both events the magnitudes available within the first hour after the event origin time severely underestimated the event size (Kerr, 2005; PTWC, 2006a). There are a number of procedures for rapid analysis of large earthquakes in use at earthquake and tsunami monitoring centers. For example, the Pacific Tsunami Warning Center uses the M_{wp} moment magnitude (Fig.1; e.g. Tsuboi *et al.*, 1999) and the M_m mantle magnitude. Currently, however, the earliest accurate estimates of the size of large earthquakes are moment tensor determinations, including the Global Centroid-Moment Tensor (CMT) (e.g. Dziewonski *et al.*, 1981), based on long-period, S and surface-wave recordings, typically not available until an hour or more after OT.

Seismic P waves are the earliest signal to arrive at seismic recording stations. At teleseismic distances the arrival times of the initial P -wave are used routinely to locate the earthquake hypocentre within about 15 minutes after OT. The P -waves also contains comprehensive information about the event size and source character. Bormann and Wylegalla (2005) and Bormann *et al.* (2006) calculate a cumulative m_b magnitude, mBc , by summing up the peak velocity amplitudes for all pulses (signal between two consecutive zero crossings) in the P waveform. Hara (2007) combines measures of the high-frequency duration and maximum displacement amplitude of P -waveforms for a set of large, shallow earthquakes to determine an empirical relation for moment magnitude. Lomax *et al.* (2007) use teleseismic P -wave signals to estimate radiated seismic energy, E , and source duration, T_0 , and show that an energy-duration moment relation, $M_{w,ED}^{10} \propto E^{1/2} T_0^{3/2}$, gives a moment magnitude, $M_{w,ED}$, that matches closely $M_{w,CMT}$ for a set of recent, large earthquakes.

Here we introduce a rapid and robust, duration-amplitude procedure to obtain an earthquake moment and a moment magnitude, M_{wps} , from P -wave recordings at teleseismic distances. This methodology can be viewed as an extension of the M_{wp} moment-magnitude algorithm.

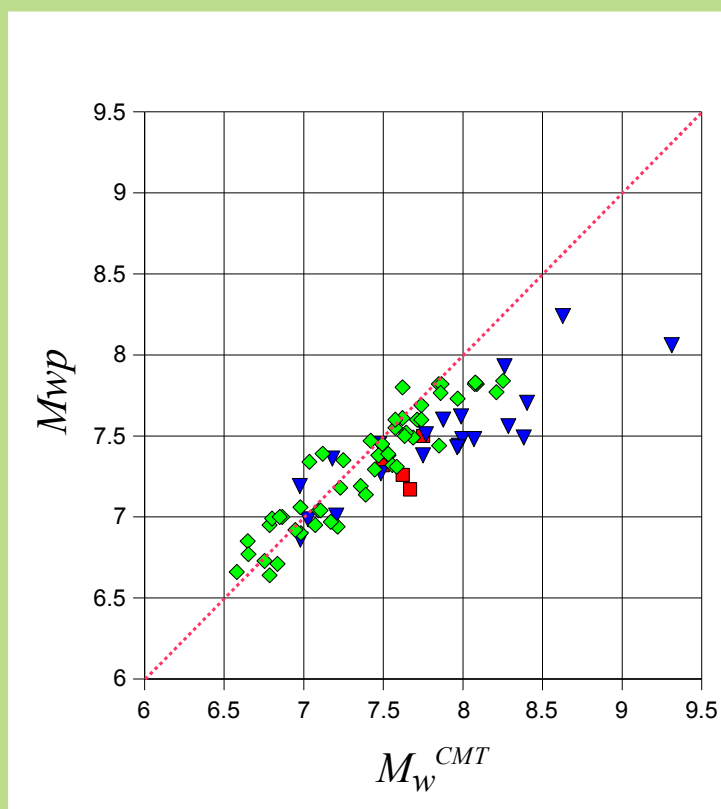


Figure 1.

M_{wp} magnitudes determined following the procedure described by Tsuboi *et al.* (1999) compared to CMT magnitude $M_{w,CMT}$ for the studied events.

Event symbols are: interplate thrust events (blue triangles); tsunami earthquakes (red squares); other event types (green diamonds). In this and the following figures the value $M_{w,CMT}=9.3$ for 2004.12.26 Sumatra-Andaman is from Tsai *et al.* (2005).

2. Methodology

Given the far-field, P -displacement waveform, $u(t)$, for an earthquake source of duration, T_0 , then a theoretical expression for the scalar, seismic moment, M_0 , is,

$$M_0 = C_M \int_{t_P}^{t_P + T_0} u(t) dt, \quad (1)$$

where t_P is the P arrival time, $u(t)$ is corrected for geometrical spreading and attenuation, and C_M is a constant that depends on the density and wave speed at the source and station, a double-couple radiation pattern and other factors.

To make further use of Eq. (1) to obtain more accurate, rapid moment-magnitude estimates, we first examine moments, \hat{M}_0 , and magnitudes, M_{wp} , determined through application to teleseismic P -displacement seismograms of a modified form of Eq. (1),

$$\hat{M}_0 = k C_M \text{Max} \left[\int_{t_P}^{t_P + T_0} |u(t)| dt, \int_{t_P}^{t_P + T_0} |u(t)| |dt| \right]. \quad (2)$$

The modifications in Eq. (2) includes the following: 1) The integral in Eq. (1) is taken separately over the positive, $u^+(t)$, and the absolute value of negative, $|u^-(t)|$, displacement amplitudes to help separate the direct P waves from surface reflection phases and other phases with opposite polarity; the maximum of these two integrals is used to calculate the moment estimate. 2) A regression constant, k , is included to compensate for unknown errors and biases in the terms of C_M and in the correction of $u(t)$ for attenuation and geometrical spreading. In addition, the source duration, T_0 , is estimated through measures on high-frequency, P -wave seismograms (Lomax, 2005; Lomax *et al.*, 2007) and T_0 is explicitly used to define the upper limit of integration. Application of the standard moment-magnitude formula, $M_w = (\log_{10} M_0 - 9.1) / 1.5$, using \hat{M}_0 and averaging over stations using robust statistics gives a P -wave moment magnitude, M_{wps} , for an event.

Estimating the source duration T_0

To estimate the source duration, T_0 , we make three assumptions: 1) the radiated P -waves contain higher frequencies than other wave types; 2) this signal can be isolated on the seismograms; 3) a meaningful time for the end of this signal can be determined. We estimate the source duration, T_0 , for each station using vertical-component seismograms and the following procedure (see Fig. 2), based on that of Lomax (2005) and Lomax *et al.*

al. (2007): 1) Convert each seismograms to high-frequency records using a narrow-band, Gaussian filter of the form $e^{-\alpha|f-f_{cent}|/f_{cent}}$, where f is frequency, $f_{cent} = 1.5$ Hz the filter center frequency, and $\alpha = 20.0$ sets the filter width. 2) Convert the high-frequency seismogram to velocity-squared time-series. 3) Smooth the velocity-squared time-series with a 10 sec wide, triangle function to form a station envelope function. 4) Measure the set of time delays after the P time at which the envelope function last drops below 90% (T_{90}), 80% (T_{80}), 50% (T_{50}) and 20% (T_{20}) of its peak value. 5) Calculate the apparent source duration, T_0 , for the station using the following algorithm, $T_0 = (1-w)T_{90} + wT_{20}$, where the weight $w = [(T_{90} + T_{20}) / 2 - 20 \text{ sec}] / 40 \text{ sec}$, with limiting values $0 \leq w \leq 1$.

Duration-amplitude moment and magnitude calculation

We evaluate the seismic moment, M_0^{pr} , for each station using vertical-component seismograms and the following procedure (see Fig. 2): 1) Bandpass from 1 to 200 sec, remove the instrument response and apply geometrical spreading and attenuation corrections to convert each seismogram to amplitude corrected, ground displacement. 2) Cut each seismogram from 10 seconds before the P -arrival to the P -arrival time plus the source duration, T_0 , or to 10 seconds before the S arrival, whichever is earlier, to obtain P -wave seismograms. 3) Apply Eqs. (2) and (4a or 4b) to each P -wave seismograms to obtain station moment estimates. We calculate an average M_0^{pr} and associated standard deviation for each event by taking the geometric mean and geometric standard deviation of the station moment estimates using robust statistics. We calculate the duration-amplitude magnitude, M_{wps} , through application of the standard moment to moment magnitude relation.

Application of the duration-amplitude procedure require seismograms, a hypocentre location and P and S travel times from the hypocentre to each station; currently, monitoring agencies have this information within about 10 minutes of OT for teleseismic events (great-circle distance (GCD) to recording stations $> -30^\circ$).

We note here that the amplitude correction of the displacement waveforms for attenuation and geometrical spreading and the calculation of C_M make use of the PREM model (Dziewonski and Anderson, 1981) without a crust (hereinafter referred to as PREM-NC), since most large events occur in oceanic regions. For shallow continental events, the effect of the crust on C_M is introduced as a magnitude correction using the PREM properties for the lower crust. Also, the radiation pattern factor in C_M for strike-slip events, which differs from that for all other event types, is determined empirically.

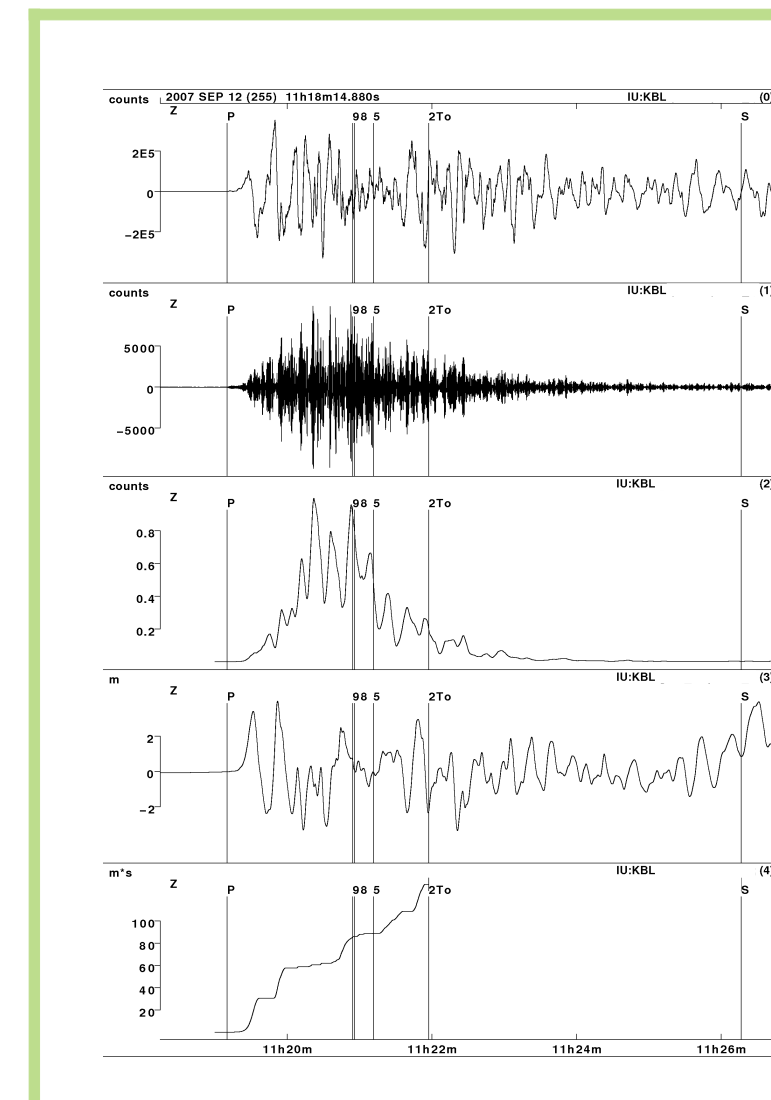


Figure 2.

Duration-amplitude processing steps for the 12 September 2007, M8.4 Sumatra earthquake recorded at station IU:KBL at 49° GCD to the northwest of the event.

Trace (0): raw, velocity seismogram;

Trace (1): 1.5 Hz, Gaussian-filtered seismogram;

Trace (2): smoothed, velocity-squared envelope;

Trace (3): amplitude-corrected, ground-displacement seismogram;

Trace (4): integral of trace (3) over the source duration using Eq. (2), note that the integral only accumulates for positive values of displacement in trace (3).
 P and S indicate the PREM-NC predicted arrival times for the first arriving, P and S waves from the hypocentre. 9, 8, 5 and 2 indicate the times at which the envelope function, trace (2), last drops below 90% (T_{90}), 80% (T_{80}), 50% (T_{50}) and 20% (T_{20}) of its peak value, respectively; T_0 indicates the estimated apparent duration, T_0 , for this station.

3. Application to recent large earthquakes

We apply the duration-amplitude methodology to 79 recent earthquakes with $M_{w,CMT}$ 6.6 to 9.3. A comparison of the obtained M_{wps} magnitudes with $M_{w,CMT}$ (Fig. 3) shows that M_{wps} matches closely $M_{w,CMT}$ up to $M_{w,CMT} = 7.5$, but with increasing magnitude M_{wps} tends to increasingly underestimate $M_{w,CMT}$. A similar result as obtained for M_{wp} (Fig. 1), though M_{wp} gives an even larger underestimate than based on M_{wps} above $M_{w,CMT} \sim 7.5$, primarily because M_{wp} only considers the first part of the P wave train while M_{wps} is based on the full interval of duration T_0 after the P arrival. Close examination of Fig. 3 shows that the trend of increasing underestimate of $M_{w,CMT}$ by M_{wps} (i.e. $\Delta M = M_{wps} - M_{w,CMT}$ becomes more negative) with increasing $M_{w,CMT}$ occurs mainly for interplate thrust earthquakes (blue triangles). M_{wps} agrees well with $M_{w,CMT}$ for most events of other types, though the lack of large events of tsunami (red squares) prevents excluding that this types follow a trend similar to that of interplate thrust earthquakes.

Thus we find for larger ($M_{w,CMT} > 7.5$) interplate thrust events that the moments determined from the P -wave train through application of Eq. (2) underestimate the corresponding CMT moments, derived from inversion of long period S and surface waves.

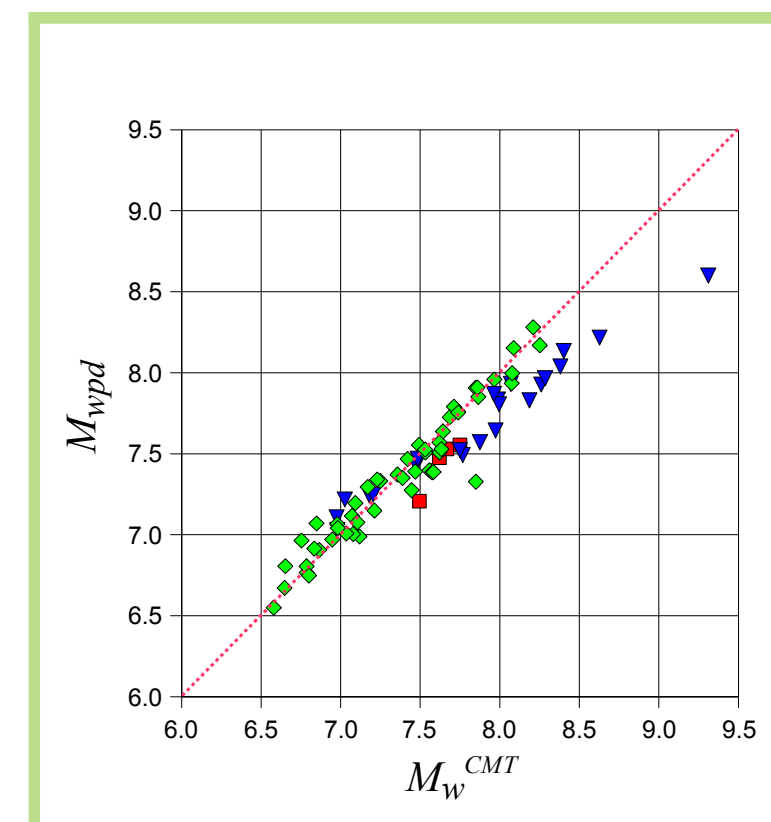


Figure 3.

Duration-amplitude magnitude M_{wps} compared to CMT magnitude $M_{w,CMT}$ for M_{wps} with no moment scaling for interplate thrust or tsunami events (i.e., application of Eq. 3) for the studied events.

Event symbols and labels as in Fig. 2. Material properties at the source are corrected to correspond to the PREM values at the CMT centroid depth. The regression against $M_{w,CMT}$ to determine k in Eq. (2) is performed excluding interplate thrust and tsunami events.

4. Moment scaling for interplate thrust and tsunami earthquakes

The variation of $\Delta M = M_{wps} - M_{w,CMT}$ differences for interplate thrust earthquakes as a function of $M_{w,CMT}$ (Fig. 3) and a similar variation as a function of M_{wps} suggest that more accurate moment estimates for these events, M_0^{pr} , can be obtained by scaling \hat{M}_0 with a factor composed of \hat{M}_0 raised to some power, i.e.,

$$\hat{M}_0' = \hat{M}_0 |\hat{M}_0 / M_0^{cent}}|^k, \quad (3)$$

where \hat{M}_0 is given by Eq. (2) and M_0^{cent} is a constant cutoff moment below which the scaling is not applied.

We also apply the moment scaling, Eq. (3), to tsunami earthquakes, since these events fall within the trend of ΔM differences for interplate thrust earthquakes (Fig. 3) and because it is difficult to distinguish these two types of events in near real-time analysis. Application of the standard moment-magnitude formula and averaging over stations gives the corresponding P -wave moment magnitude, M_{wps} .

Application of Eq. (3) to the interplate thrust and tsunami events from the set of studied earthquakes gives $R=0.4$ and $M_0^{cent}=7.5 \times 10^{19}$ N-m (equivalent to $M_w=7.2$) for the best match of M_{wps} to $M_{w,CMT}$. Thus we arrive at a preferred, duration-amplitude expression for moment estimation,

$$\hat{M}_0' = \hat{M}_0 |\hat{M}_0 / M_0^{cent}}|^k, \quad (4a)$$

for interplate thrust and tsunami events when $\hat{M}_0 \geq M_0^{cent}$, and

$$\hat{M}_0' = \hat{M}_0, \quad (4b)$$

otherwise, where \hat{M}_0 is given by Eq. (2) with $C_M=1.62 \times 10^{19}$ and $k=1.1$. M_{wps} magnitudes determined using Eqs. (4a), (4b) and (2) for the studied earthquakes match closely $M_{w,CMT}$ for all event types at all magnitudes (Fig. 4).

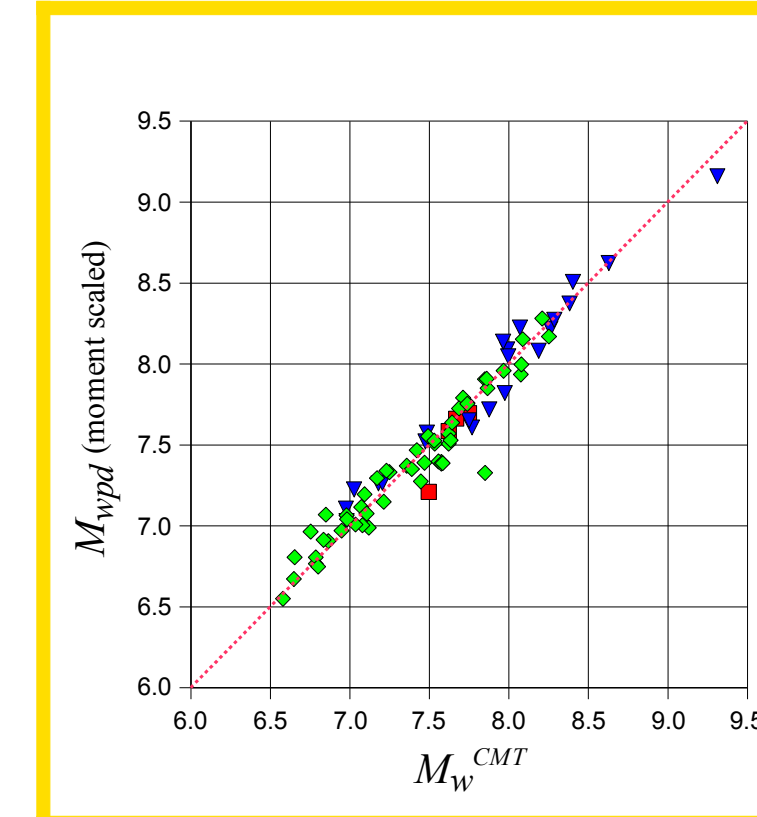


Figure 4.

Duration-amplitude magnitude M_{wps} compared to CMT magnitude $M_{w,CMT}$ for M_{wps} corrected with moment scaling for interplate thrust and tsunami events (i.e., application of Eqs. 2 and 4a or 4b) for the studied events.

Event symbols and labels as in Fig. 2. Material properties at the source are corrected to correspond to the PREM values at the CMT centroid depth. The regression against $M_{w,CMT}$ to determine k in Eq. (2) is performed excluding interplate thrust and tsunami events.

5. Energy-to-moment ratio Θ

The energy-to-moment ratio parameter, Θ , (e.g., Newman, and Okal, 1998) for identification of tsunami earthquakes is defined as $\Theta = \log_{10} E / M_0$, where E is the radiated seismic energy and M_0 the moment. From duration-amplitude estimates of moment, M_0^{pr} , and duration, T_0 , we can obtain Θ through application of the energy-duration relation of Lomax *et al.* (2007), $M_{w,ED}^{10} = c E^{1/2} T_0^{3/2}$, where $c = 1.55 \times 10^{16}$ for average crust - upper mantle material properties. Substituting M_0^{pr} for $M_{w,ED}$ in Equation 7, solving for E and substituting into the definition of Θ , we get,

$$\Theta = \log_{10} (c^{-2} M_0^{pr} / T_0^3). \quad (5)$$

Θ values determined using Eq. (5) for the studied earthquakes are plotted in Fig. 5 as function of $M_{w,CMT}$.

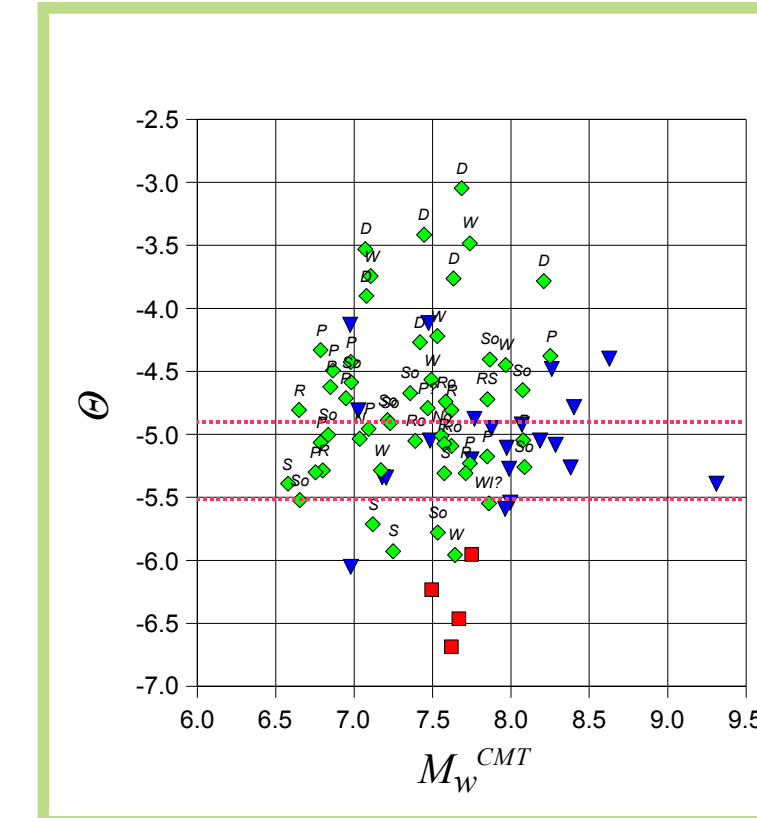


Figure 5.

Θ values from application of Eq. (5) to duration-amplitude results with moment scaling for interplate thrust and tsunami events (i.e., application of Eqs. 2 and 4a or 4b) for the studied events.

Θ values are plotted against CMT magnitude $M_{w,CMT}$. Lines of constant Θ are shown for $\Theta = -4.9$, an expected value for all earthquakes, and $\Theta = -5.5$ - below which indicates a possible tsunami earthquake. Event symbols and labels as in Fig. 1. Earthquake types: I - interplate thrust; T - tsunami earthquake; W - down-dip; P - intraplate; D - deep; So - strike-slip oceanic; Ro - reverse-faulting oceanic; No - normal-faulting oceanic; S - strike-slip continental; R - reverse-faulting continental; N - normal-faulting continental.

6. Discussion

We have introduced a duration-amplitude procedure to obtain rapidly an earthquake moment, M_0^{pr} , and moment magnitude, M_{wps} , from P -wave recordings at teleseismic distances. Because the required recordings are available in near-real time at earthquake and tsunami monitoring centers, M_{wps} can be available within about 20 minutes after OT. For major and great earthquakes ($M_{w,CMT} \geq 7.0$), M_{wps} (with moment scaling for interplate thrust and tsunami events) matches $M_{w,CMT}$ typically within ± 0.2 magnitude units, with a standard deviation of only $\sigma = 0.10$ (Fig. 4). In addition, M_{wps} does not exhibit saturation for the largest events, or, equivalently, $\Delta M = M_{wps} - M_{w,CMT}$ does not decrease with increasing $M_{w,CMT}$. Thus M_{wps} equals or outperforms other procedures for rapid moment magnitude determination.

The improved agreement between M_{wps} and $M_{w,CMT}$ relative to other rapid procedures, including M_{wp} , can be attributed primarily to the use in Eq. (2) of the full t_P to $t_P + T_0$ interval for integration with testing of integrals over positive and negative values of displacement, and to the application of the moment scaling, Equation (4a), for interplate thrust and tsunami earthquakes. These characteristics of the duration-amplitude procedure show that it is an extension of the M_{wp} moment-magnitude algorithm, recalling also that both procedures are ultimately based on Eq. (1).

Energy-to-moment ratio Θ

The duration-amplitude results provide a rapid estimate (Eq. 5) of the energy-to-moment ratio Θ used for identification of tsunami earthquakes. The duration-amplitude estimates of Θ (Fig. 5) are $\Theta \leq -5.9$ for all tsunami earthquakes, facilitating identification of these events. Some interplate thrust events and many strike-slip events have low Θ values below -5.5, and most deep events have high Θ values. The low values of Θ for some strike-slip earthquakes can be attributed to overestimate of T_0 for the smaller events, or to anomalously low amplitudes in the P wave train due to the strike-slip radiation pattern. A small error in T_0 can give a large error in Θ , since Θ is proportional to T_0^3 (Eq. 5).

Identification of interplate thrust, tsunami and other event types

Even without the moment scaling M_{wps} provides a closer match to $M_{w,CMT}$ magnitude, including for larger interplate thrust events and tsunami earthquakes, than do most other procedures for rapid magnitude estimation (standard deviation of $\sigma = 0.16$; cf. Fig. 3). And a "raw" M_{wps} given by direct application of Eq. (2) without any corrections for event type (e.g., no crustal correction for shallow continental events, no correction for radiation pattern for strike-slip events) still matches $M_{w,CMT}$ with $\sigma = 0.16$. However, to obtain the best match of M_{wps} to $M_{w,CMT}$ requires identification of interplate thrust and tsunami earthquakes for application of the moment scaling, and further classification by event type, e.g., as continental, oceanic, strike-slip, or deep, for application of corrections for PREM properties at the source depth and for radiation pattern. In practice, information on the location, tectonic setting and likely focal mechanism of an event will usually be available before the duration-amplitude analysis is completed, thus likely interplate thrust and tsunami events, the event type and the approximate source depth can be identified rapidly.

Application at local and regional distances

It is likely that the duration-amplitude methodology can be applied at local and regional distances, i.e. $GCD < 30^\circ$, thus reducing the time delay after OT for obtaining event size estimates. The main difficulty in applying the methodology for seismograms recorded at $GCD < 30^\circ$ is that significant S signal may remain on the high-frequency, P -wave seismograms used for determination of the duration, T_0 , which complicates the analysis of larger events. In this case, the direct P -wave radiation can often be isolated by applying the narrow-band, Gaussian filtering at higher frequencies (e.g., 5-20 Hz), but this requires that high dynamic-range, high sample-rate data is available.

Physical implications of the M_{wps} moment scaling

The increasing underestimate of $M_{w,CMT}$ with increasing magnitude by unscaled M_{wps} for interplate thrust (and possibly tsunami) earthquakes (Fig. 3) and the consequent need for a moment scaling (Eq. 4a) may have important physical implications. The increasing underestimate of $M_{w,CMT}$ is probably not due to station site or path effects, since then it would occur for all event types, and it is probably not a direct effect of the source mechanism radiation pattern, since then it would vary with event size. Examination of M_{wps} estimates obtained with different long-period cutoffs indicates that the increasing underestimate of $M_{w,CMT}$ is not due to magnitude saturation. Thus the increasing underestimate of $M_{w,CMT}$ may be associated with near-source, dynamic phenomena unique to larger, shallow interplate thrust (and possibly tsunami) earthquakes. The form of the moment scaling, Eq. (4a), suggests a deficiency that increases with event size in the amplitude of far-field, radiated P -waves relative to the amplitudes expected from the CMT results. The destructive interference of pP or sP waves with direct, down-going P waves is an often cited explanation for reduced, far-field P amplitudes, but this is a kinematic mechanism which must be cast into a dynamic framework for large, shallow earthquakes where the interference would occur within the rupture volume and simultaneous with rupture. The deficiency in amplitude must therefore be associated with a near-field mechanism which reduces the radiated kinetic energy while maintaining the seismic energy balance.

Acknowledgements

This work benefited greatly from discussions with Massimo Cocco, Paul Earle, Goran Ekström, Barry Hirshorn, Chris Marone, Stefan Nielsen, and Martin Vallée. The work of A.L. was supported by personal funds, A.M. has been supported by the INGV-DPC (Dipartimento della Protezione Civile) S4 project - "Stima dello scuotimento in tempo reale e quasi-reale per terremoti significativi in territorio nazionale". The IRIS DMC (<http://www.iris.edu>) provided access to waveforms used in this study.

References

- Bormann, P. and K. Wylegalla, 2005. Quick Estimator of the Size of Great Earthquakes, *Eos Trans. AGU*, **86**(46), 464.
- Bormann, P., K. Wylegalla and J. Saul, 2006. Broadband body-wave magnitudes mB and mBe for quick reliable estimation of the size of great earthquakes, *USGS Tsunami Sources Workshop 2006*, poster, http://spring.msi.unn.edu/USGS/Posters/Bormann_et_al_poster.pdf.
- Dziewonski, A.M. and D.L. Anderson, 1981. Preliminary Reference Earth Model (PREM), *Phys. Earth Planet. Inter.* **25**, 297-356.
- Dziewonski, A., T.A. Chou, and J. H. Woodhouse, 1981. Determination of earthquake source parameters from waveform data for studies of global and regional seismicity, *J. Geophys. Res.*, **86**, 2825-2852.
- Hara, T., 2007. Measurement of the duration of high-frequency energy radiation and its application to determination of the magnitudes of large shallow earthquakes, *Earth Planets Space*, **59**, 227-231.
- Lomax, A., 2005. Rapid estimation of rupture extent for large earthquakes: application to the 2004, M9 Sumatra-Andaman mega-thrust. *Geophys. Res. Lett.*, **32**, L10314, doi:10.1029/2005GL022437.
- Lomax, A., A. Michelini and A. Piatanesi, 2009. An energy-duration procedure for rapid determination of earthquake magnitude and tsunamigenic potential, *Geophys. J. Int.*, **NN**, nnn-nnn, doi:10.1111/j.1365-246X.2007.03469.x
- Kerr, R.A., 2005. Failure to gauge the quake crippled the warning effort, *Science*, **307**, 201.
- Newman, A.V., and E.A. Okal, 1998. Teleseismic Estimates of Radiated Seismic Energy: The E/M_0 Discriminant for Tsunami Earthquakes, *J. Geophys. Res.*, **103** (11), 26,885-98.
- PTWC, 2006a. Tsunami Bulletin Number 001, Issued at 0836Z 17 Jul 2006, *Pacific Tsunami Warning Center/NOAA/NWS*.
- PTWC, 2006b. Tsunami Bulletin Number 002, Issued at 1108Z 17 Jul 2006, *Pacific Tsunami Warning Center/NOAA/NWS*.
- Tsai, V.C., M. Nettles, G. Ekström, and A.M. Dziewonski, 2005. Multiple CMT source analysis of the 2004 Sumatra earthquake, *Geophys. Res. Lett.*, **32**, L17304, doi:10.1029/2005GL023813.
- Tsuboi, S., P. M. Whitmore, and T. J. Sokolowski, 1999. Application of M_{wp} to deep and teleseismic earthquakes, *Bull. Seism. Soc. Am.*, **89**, 1345-1351.